22. Vaysenzee K., Pol'te G. A., Lins G. Avtomatizirovannoe opredelenie pogreshnosti geometricheskih izmereniy // Izvestiya vysshih uchebnyh zavedeniy. Priborostroenie. 2011. Vol. 54, Issue 12. P. 47–49.

23. Teoriya i pryntsypy pobudovy avtomatyzovanoi systemy dlia liniynykh i kutovykh peremishchen obiektiv vyrobnytstva z vykorystanniam matematychnoho aparatu kvaternioniv i elementiv shtuchnoho intelektu: monohrafiya / Cherepanska I. Yu. Kyrylovych V. A., Bezvesilna O. M., Sazonov A. Yu. Zhytomyr: ZhDTU, 2016. 326 p.

24. Cherepanska I. Yu., Bezvesilna O. M., Sazonov A. Yu. Sposib vymiriuvannia kutiv: Pat. No. 124155 UA. No. 201709792; declareted: 09.10.2017; published: 26.03.2018, Bul. No. 6.

25. Rojas R. Neural Networks. A Systematic Introduction. Springer-Verlag Berlin Heidelberg, 1996. 502 p.

26. D'yakonov V. P., Kruglov V. V. Matlab 6.5 SP1/7/7 SP1/7 SP2 + Simulink 5/6. Instrumenty iskusstvennogo intellekta i bioinformatiki. Moscow: SOLON-PRESS, 2006. 456 p.

Запропоновано систему ранньої вібраційної діагностики газоперекачувальних агрегатів, а саме підшипникових вузлів з покращеними метрологічними характеристиками. Спосіб дозволяє вирішувати задачу раннього діагностування підшипників кочення при несприятливих умовах застосування. Дослідження показали, що це досягнуто завдяки використанню слідкуючих режекторних фільтрів на базі N-канальних структур з використанням ітераційних-інтегруючих перетворювачів. Результати моделювання 4-ох канального фільтра, при реальних вхідних сигналах підшипникових пошкоджень, показали його дієздатність. На цій основі була створена підсумкова модель вихідного сигналу фільтра. Представлена функціональна схема детектора середньоквадратичних значень з моделю вихідного сигналу слідкуючого режекторного фільтра при реальних вхідних сигналах. Для створення моделі сигналу на вході детектора середньоквадратичних значень були визначені реакції фільтра на кожну частоту яка відповідає за певне пошкодження. Час аналізу вибрано так, щоб він був рівний періоду мінімальної частоти биття, тобто T_a=164 мс (для підшипника типу 222).

Досліджено ефективність пристрою шляхом моделювання пошкоджень реального підшипника газотурбінного двигуна. Запропонована методика аналізу та узагальнений вібродіагностичний критерій, який дає можливість врахувати степінь навантаження двигуна. Це підвищує точність та достовірність попереднього аналізу при діагностуванні підшипника кочення на стадії зародження пошкодження.

Наведено характеристики електрометричного вимірювального підсилювача для роботи з п'єзоелектричними датчиками та запропонованого зарядового вимірювального підсилювача для роботи з п'єзоелектричними датчиками. При умові розбалансу вхідної ланки, що зумовлено не ідентичністю паразитних ємностей вхідного кабелю. Показано, що проникнення мережевої завади на вихід зарядового вимірювального підсилювача, забезпечує на два порядки краще співвідношення сигнал/шум ніж у електрометричного вимірювального підсилювача

Ключові слова: вібраційна діагностика, газотурбінний двигун, диференціальний зарядовий підсилювач, підшипниковий вузол, слідкуючий режекторний фільтр

DEVELOPMENT OF THE SYSTEM FOR VIBRATION DIAGNOSIS OF BEARING ASSEMBLIES USING AN ANALOG INTERFACE

V. Dovhan
Deputy Head
Scientific and Research Department
of Measurements of Electrical and
Magnetic quantities measurements
SE «UKRMETRTESTANDART»
Metrologichna str., 4, Kyiv, Ukraine, 03143
E-mail: dovgan_csm@ukr.net

V. Kvasnikov
Doctor of Technical Sciences, Professor,
Head of Department
Department of Computerized Electrical
Systems and Technologies*

D. Ornatskiy
Doctor of Technical Sciences, Associate
Professor, Head of Department
Department of Information
and Measuring Systems*
*National Aviation University
Kosmonavta Komarova ave., 1, Kyiv,
Ukraine, 03058

1. Introduction

At present, there is a pressing issue related to the improvement of reliability of the gas transportation system of Ukraine (GTU), which is one of the major national achievements. Gas-turbine engines (GTE) are the most responsible functional nodes in GTU. Requirements aimed at improving the reliability and durability of structural elements and units

of GTE become stricter, necessitating the improvement of methods and means to estimating the current technical condition of engine during its operation.

One of the key elements of GTE is bearing nodes, which, due to significant rotation frequency, employ single row roller bearings. The operability of bearings and their residual resource in most cases determine the engine's interval between repairs.

More than 40–50 % of GTE failures occur due to defective bearing assemblies. The systems to protect the engine from global damage and its break in case of emergencies are applied at present. However, using such a system does not make it possible to exactly estimate the state of a bearing at an early stage of defect development [1].

The relevance of the issue is related to the fact that the task on determining the damage to bearing assemblies at the early stage of its development is inefficiently resolved today. The most common technique is to use the Discrete Fourier transform (DFT), which is known to diminish its effectiveness in the presence of significant noise and interference. Another trend is the use of digital filters of high orders, however, their quick and accurate readjustment under specified conditions is also a problem (the signal/noise ratio is significantly less than 1).

2. Literature review and problem statement

At present, the following methods are widely used for diagnosing bearing assemblies in GTE: a method of Peak-factor, a method of direct spectrum, an envelope spectrum method, and a method of shock pulses. However, the above-mentioned methods have a number of disadvantages. The disadvantage of the application of the Peak-factor method for solving a task on the early diagnosis of roller bearings is the low noise resistance, which requires placing the sensor directly on the bearing, which is impossible in practice [2]. The same shortcoming is inherent in the method of the excess [1]. The drawback of the method of shock pulses is the blurred spectrum at changing the speed of shaft rotation, which could lead to the disappearance of the discrete components of the spectrum [3]. The same shortcoming characterizes digital spectrum analyzers based on FFT (Fast Fourier transform) [4].

In order to run a vibration analysis of bearing assemblies in GTE, piezoelectric accelerometers are applied in most cases, which have a number of advantages such as low cost, reliability, and durability [3], however, one of the main problems of their application is the existence of powerful disturbances and network interference. It is also possible to use optical vibration sensors (triangulation sensors of PSD type), but their use is limited by the high cost and setting complexity. One can use electromechanical vibration sensors; however, they demonstrate low reliability due to the presence of moving parts.

There are methods that are based on the use of narrow-band tracking selective filters (or time averaging [3]). Their metrological characteristics do not always meet the criteria for measuring useful signals against the background of strong interference, caused by the close spaced rotor harmonics [5–7].

The use of digital filters of high orders under conditions for the need to track the frequency of useful signal that changes is limited by the complexity of fast and accurate measurement of the useful signal frequency under conditions of strong interferences (the signal to noise ratio is less than 1). As well as by the fact that the frequency that corresponds to the defects of bearings fluctuates randomly [8].

Another problem is the compromised effectiveness of existing methods of diagnosis under actual measurement conditions (a change in the signal/noise ratio is predetermined by a change in GTE load and a change in the shaft rotation frequency) [1].

The effectiveness of the use of deterministic methods at diagnosing decreases because the vibrations of bearings are of a random character. This randomness manifests itself in the fluctuations of bearing frequencies. In addition, the vibrations of a bearing at the point of registration are affected by vibrations and noise from other nodes in a running engine, which can exceed the useful signal by 1,000 times.

The most common among the deterministic methods for diagnosis of bearing assemblies are the spectral methods, based on a spectral analysis of vibrograms using the discrete Fourier transform (DFT). An increase in the efficiency of DFT at adverse signal to noise ratio is considered in [9]. It is shown that at the signal to noise ratio of 40 dB it is possible, by using the Harris weight function, to determine a component with a frequency at a distance of 60 % from the more powerful harmonics; however, under actual conditions the bearing frequencies can be located closer to the powerful harmonics at a distance of 10–20 %. In this case, the weight function method will not produce the expected result.

Statistical methods, such as the Kurtosis factor, SpikeEnergy (splash energy – SE) and others, perform quite successfully when there is a possibility to mount the vibration sensors directly on the bearing's casing. Under the condition for measurements at one point and diagnosing a single bearing, in all other cases, the application of these methods is problematic [1, 10, 11].

Paper [12] examined vibration diagnosis of shafts oscillations in 3 coordinates that make it possible to estimate the technical condition of bearing assemblies. The disadvantage of the method is the complexity of implementation.

Work [13] proposed an algorithm for analysis of vibrations at rotor machines in actual time. The downside is the stochastic model of the useful signal that requires the location of the sensor directly on a bearing.

[14] shows analytical methodology for diagnosing bearing assemblies under condition of change in the speed of shaft rotation. It could be effectively used for a preliminary diagnosis of transmissions and gearboxes. It is difficult to be applied for diagnosing bearing nodes due to the non-stationarity of measuring signals.

Paper [15] addresses the improvement of methods for cepstral analysis. The method is largely insensitive to a change in the phase of the examined signals and to the parameters of propagation of mechanical oscillations. It is used to diagnose reducers.

Article [16] reports modern methods for diagnosis of rotor machines. The recommendations are given to optimize the application of methods and to test new diagnostic parameters.

In [17, 18], authors improve methods of stochastic analysis based on known methods such as the Kurtosis factor.

A method for improving noise-resistance through a combination of the resonance method and the wavelet transform is given in [19]. The drawback is the complexity of implementation and high cost.

The features of GTE design, which are part of the gas-pumping units, imply that it is not possible to mount vibration sensors directly on the bearing. They are installed on rather pliable external force casings, resulting in the distortions of signals from bearings through the multitude of resonances and transitions.

These problems create complex contradictory requirements to the equipment, which makes this task relevant for measuring instruments when bearing assemblies in GTE are vibrationally diagnosed at an early stage.

3. The aim and objectives of the study

The aim of this study is to develop a system of vibration diagnosis of bearing assemblies of GTE with improved metrological characteristics for early diagnosis.

To accomplish the aim, the following tasks have been set:
– to develop and improve the structural scheme of the system for early diagnosis of damage to bearing assemblies;
– to devise a procedure for determining the time of analysis for actual input signal;
– to design and explore a circuit of the measuring charging amplifier with differential-current outputs with improved metrological characteristics to operate with piezoelectric sensors.

4. Materials and methods to study a system for vibration diagnosis of bearing assemblies

4. 1. Improved structural circuit of the system

Fig. 1 shows block diagram of the device for vibration diagnosis of bearing assemblies with improved metrological characteristics [20].
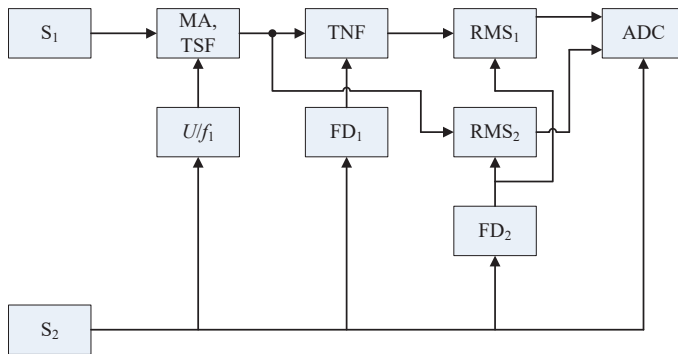

Fig. 1. Device for vibration diagnosis of bearing assemblies

The device for vibration diagnosis (Fig. 1) consists of the following units:
S_1 – piezoelectric sensor;
S_2 – optical tachometer;
MA, TSF – measuring amplifier with a built-in tracking selective (bandwidth) 1.6 octave filter;
TNF – 4-channel tracking notch filter;
RMS_1, RMS_2 – detectors of root-mean-square values;
U/f_1 – transducer frequency-voltage;
FD_1, FD_2 – frequency dividers;
ADC – analog-to-digital converter.

MA, TSF serve to suppress (decrease) network interference and to limit the band of useful signal at the level of 1.6 octaves with an increase in the coefficient of amplification on the edges of the range. To compensate for the uneven frequency response (FR) of the 4-channel filter and to take into consideration the distribution of harmonics over the spectrum of the state of roller bearings, as well as to compensate for the possible high-frequency resonances.

Subsequently, the unit of the N-channel tracking notch filter (TNF) suppresses the harmonics that are multiple to the shaft rotation speed. A diagnostic criterion is formed in ADC of the logometric type that makes it possible to reduce the influence of a load change in GTE.

The device can operate under two modes:
– the viewing mode;
– the careful mode.

The entire band of damage frequency is analyzed under the viewing mode. In this case, the bandwidth frequency of the preliminary filter MA, TSF is 1.6 octaves. In careful mode, the bandwidth of the preliminary filter MA, TSF narrows to 1.3 octaves, and under this mode, it would actually pass the signal with a frequency that corresponds to a certain damage with the traces of the closest rotary harmonics.

4. 2. Model of input (useful) signal of the diagnosing device

The output signal of sensor S_1 can be represented in the form of a Fourier series [21]:

$$U_g(t) = \sum_{n=1}^{6} A_n \sin(n\omega_0 t + \varphi_n) + \sum_{i=1}^{3} A_i \sin(\eta_i \omega_0 t + \varphi_i). \quad (1)$$

Then the output signal of the tracking selective filter takes the form:

$$U_{MA,TSF}(t) = \sum_{n=1}^{6} A_n \left| K_{MA,TSF}(n\omega_0) \right| \cdot \sin\left(\begin{matrix} n\omega_0 t + \varphi_n + \\ + \varphi_{MA,TSF}(n\omega_0) \end{matrix} \right) +$$
$$+ \sum_{i=1}^{3} A_i \left| K_{MA,TNF}(\eta_i \omega_0) \right| \cdot \sin\left(\begin{matrix} \eta_i \omega_0 t + \varphi_i + \\ + \varphi_{MA,TNF}(n\omega_0) \end{matrix} \right), \quad (2)$$

where A_n is the amplitude of the n-th harmonic (rotor frequency) at the output of the sensor; $n=2...6$ are the harmonics of rotor frequency (as estimated); $K_{MA,TSF}$ is the coefficient of transmission of the tracking band filter; A_i are the amplitudes of spectral components of bearing's damage; $i=1, 2, 3$ is the number of frequency, which is responsible for a certain damage; φ_n, φ_i are the initial phases of respective harmonics at the output of the filter; $\varphi_{MA,TNF}$ is the phase shift introduced by the filter at this frequency; ω_0 is the shaft (rotor) rotation frequency; η_i is the damage coefficient of a roller bearing [3]; $i=1, 2, 3$.

Table 1

Damage coefficients of a roller bearing

Damage coefficient	Title	Calculation formula
η_1	Damage coefficient of the bearing's inner ring	$\eta_1 = \dfrac{N}{2}\left(1 + \dfrac{B_d}{P_d}\cos\varphi\right)$
η_2	Damage coefficient of the bearing's outer ring	$\eta_2 = \dfrac{N}{2}\left(1 - \dfrac{B_d}{P_d}\cos\varphi\right)$
η_3	Damage coefficient of the bearing's roller bodies	$\eta_3 = \dfrac{P_d}{2 \cdot B_d}\left(1 - \left(\dfrac{B_d}{P_d}\cos\varphi\right)^2\right)$

Notes: N is the number of roller bodies; B_d is the diameter of roller bodies; P_d is the mean diameter of the roller bearing; φ is the angle of contact

We shall obtain signals at the input of the logometric ADC that are proportional to the sum of squares of the valid values for the spectral components of input signals:

$$U_{RMS1} = K_{RMS} T_a \times$$

$$\times \left\{ \sqrt{ \sum_{i=1}^{3} \left[\begin{array}{c} A_i \left| K_{MA,TSF}(\eta_i \omega_0) \right| \times \\ \times \left| K_{TNF}(\eta_i \omega_0) \right| \end{array} \right]^2 } \right\}, \qquad (3)$$

where K_{RMS1} is the coefficient of transmission of root-mean-square values detector RMS$_1$; T_a is the time of analysis; $K_{MA,TSF}$ is the transmission coefficient of the N-channel filter at frequencies that correspond to a certain damage; K_{TNF} is the transmission coefficient of tracking notch filter.

Let us represent U_{RMS2} in the form:

$$U_{RMS2} = K_{RMS2} T_a \left\{ \sqrt{ \begin{array}{c} \sum_{i=1}^{3} \left[A_i \left| K_{MA,TSF}(\eta_i \omega_o) \right| \cdot \left| K_{TNF}(\eta_i \omega_o) \right| \right] I + \\ + \sum_{n=1}^{6} \left[A_n \left| K_{MA,TSF}(n \omega_o) \right| \right]^2 \end{array} } \right\}, (4)$$

where K_{RMS2} is the transmission coefficient of detector RMS_2.

We shall choose, as a generalized vibrodiagnostic criterion lead ratio of voltages on the outputs of SSI:

$$\theta = \frac{U_{RMS1}}{U_{RMS2}}. \qquad (5)$$

Given that $RMS_1 \approx RMS_2$, and $\sum_{n=1}^{6} \gg \sum_{i=1}^{3}$, expression (5) takes the form:

$$\theta = \sqrt{ 1 + \frac{\sum_{i=1}^{3} [A_i \left| K_{MA,TSF}(\eta_i \omega_o) \right| \cdot \left| K_{TNF}(\eta_i \omega_o) \right|] I}{\sum_{n=1}^{6} [A_n \left| K_{MA,TSF}(n \omega_o) \right|] I} } \qquad (6)$$

or

$$\theta - 1 \approx 0.5 \frac{\sum_{i=1}^{3} [A_i \left| K_{MA,TSF}(\eta_i \omega_o) \right| \cdot \left| K_{TNF}(\eta_i \omega_o) \right|] I}{\sum_{n=1}^{6} [A_n \left| K_{MA,TSF}(n \omega_o) \right|] I}. \qquad (7)$$

Important here is to select the time of analysis T_a. Control over MA, TNF is executed using a sensor of the GTE shaft rotation speed, which, it is advisable, an optical tachometer and a voltage-frequency converter to control the universal filter, driven by voltage. Frequency dividers with division coefficients n and m are required to obtain the signals of TNF synchronization and to form the time of analysis T_a, respectively. If one denotes the GTE shaft rotation frequency conversion coefficient of sensor S_2 as K$_1$, then the dividing coefficient n in divider FD_1 can be represented in the following form:

$$n = \frac{K_1}{4}, \quad m = \frac{K_1 f_{0min}}{f_{minb}}, \qquad (8)$$

where f_{minb} is the minimum beat frequency to be determined by the distribution of spectral components of the useful signal; f_{0min} is the minimum speed of rotor rotation.

The model of the useful signal was constructed, which consists of 3 generators with the frequencies that correspond to the roller bearing's damage, which is applied in the NK-12ST GTE (type 222) [1].

4. 3. Calculation of frequencies that correspond to the damage to bearings

Results of calculating the damage coefficients for the actual roller bearing used in the NK-12ST GTE are given in Table 2.

Table 2

Damage coefficients

Type of bearing	Damage coefficient of the bearing's inner ring η_1	Damage coefficient of the bearing's outer ring η_2	Damage coefficient of balls η_3	P_d, mm	B_d, mm	N, units	Angle, °
222	5.92	4.08	2.62	155	28.58	10	0±20°

Notes: P_d is the mean diameter; B_d is the diameter of rolling bodies; N is the number of rolling bodies

The calculation of frequencies that correspond to the damage to the bearing (222):
– the frequency of damage to the inner ring is:

$5.92 \cdot (102.5 – 142) = 606.8 – 840.6$ Hz;

– the frequency of damage to the outer ring is:

$4.08 \cdot (102.5 – 142) = 418.2 – 579.4$ Hz;

– the frequency of damage to the rolling bodies is:

$2.62 \cdot (102.5 – 142) = 268.6 – 372.0$ Hz.

The frequency of shaft (rotor) rotation in the NK-12ST GTE: $f_{min} – f_{max} = 102.5 – 142$ Hz.

5. Simulation and research results

5. 1. Modeling the 4-channel filter at actual input signals

Fig. 2 shows the functional circuit of the 4-channel filter with a coefficient of window overlap $k = 1$. The circuit is composed of cycle pulse generator G1, pulse divider on two J-K triggers, DD1 DD2, 4 iterative integrating converters implemented based on DA1...DA8, adder DA10 and an output filter. We use, as the input filter, a lower frequencies filter of second order with the Bauterworth approximation and the Salen Key type implementation actualized on DA9.

Consider the output signal of the 4-channel filter when a signal with a frequency of 268.6 Hz is sent to the input. The signal corresponds to the damage to the bodies of roller bearing at a minimum rotor rotation frequency of 102.5 Hz (corresponding to the minimum speed of shaft rotation, 6,150 rpm). We shall obtain at the outlet from the filter a signal, which consists of two harmonics of different frequency and the total amplitude of $U_{p-p} = 200$ mV.

The time diagram of the signal's output signal under these conditions is shown in Fig. 3.

The frequency of low-frequency oscillation is 14.3 Hz, amplitude 13.0 mV. The frequency of high-frequency oscillation will reach 138.0 Hz, amplitude 86.0 mV.

The high-frequency oscillation of this signal is equal to the difference between the shaft's fourth harmonic and the damage frequency of rolling bodies.

The low-frequency component of this sum is equal to the minimum beat frequency at the second and third harmonic.

In the second case, a signal with a frequency of 418.2 Hz is sent to the input, which corresponds to the damage to the outer ring of a roller bearing at the rated rotor frequency of 102.5 Hz. Frequency of synchronization is 410 Hz. Time diagram of the filter's output signal under these conditions is shown in Fig. 4.
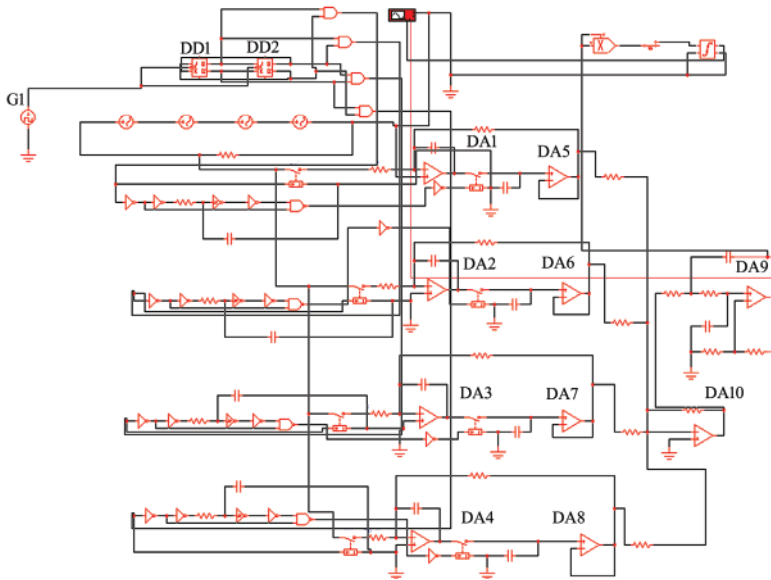
Fig. 2. Diagram of the 4-channel filter with a coefficient of window overlap k=1
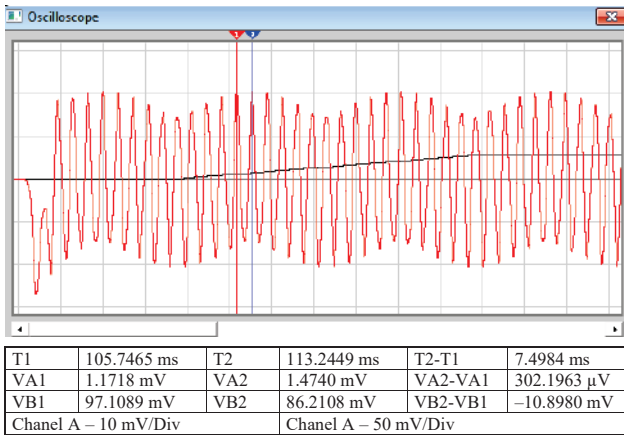

T1	105.7465 ms	T2	113.2449 ms	T2-T1	7.4984 ms
VA1	1.1718 mV	VA2	1.4740 mV	VA2-VA1	302.1963 µV
VB1	97.1089 mV	VB2	86.2108 mV	VB2-VB1	−10.8980 mV
Chanel A – 10 mV/Div			Chanel A – 50 mV/Div		

Fig. 3. Time diagram of the signal of damage to rolling bodies

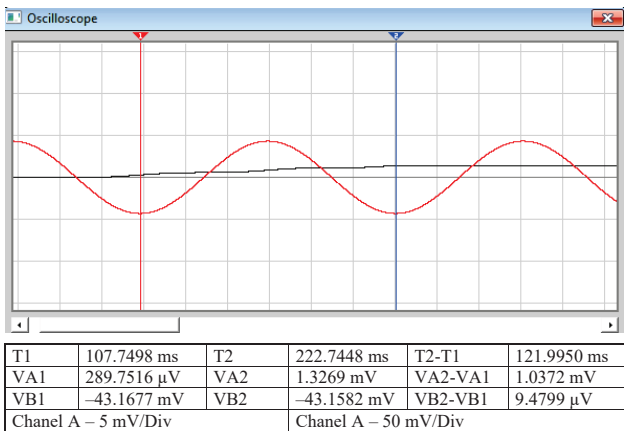| T1	107.7498 ms	T2	222.7448 ms	T2-T1	121.9950 ms
VA1	289.7516 µV	VA2	1.3269 mV	VA2-VA1	1.0372 mV
VB1	−43.1677 mV	VB2	−43.1582 mV	VB2-VB1	9.4799 µV
Chanel A – 5 mV/Div			Chanel A – 50 mV/Div		

Fig. 4. Time diagram of the signal of damage to an outer ring

At the output, an oscillation harmonic with a frequency of 8.2 Hz and an amplitude of 43.0 mV. In this case, the amplitude of the input signal is 1 V, the filter gain factor is 1 in the middle of the frequency range.

The amplitude of this original signal will be proportional to the amplitude of the input signal, that is, the intensity of damage.

In the third case, a signal with a frequency of 606.8 Hz is sent to the input, which corresponds to the damage to the inner ring of a roller bearing at the rotor's rated frequency of 102.5 Hz. Frequency of synchronization is 410 Hz. Time diagram of the filter's output signal under these conditions is shown in Fig. 5.

We observe a signal, which is equal to the product of two harmonic oscillations, the frequency of low-frequency oscillation is 8.2 Hz and the maximum total beat amplitude is 9 mV, the frequency of high-frequency oscillations is about 200 Hz. The frequency of low-frequency oscillation is equal to the difference between the sixth harmonic and the frequency of damage to an inner ring. The frequency of high-frequency oscillation is equal to the difference between the frequency of damage to an inner ring and the sixth harmonic of rotor frequency. The amplitude of pulsation is proportional to the product of root-mean-square values for input signals.

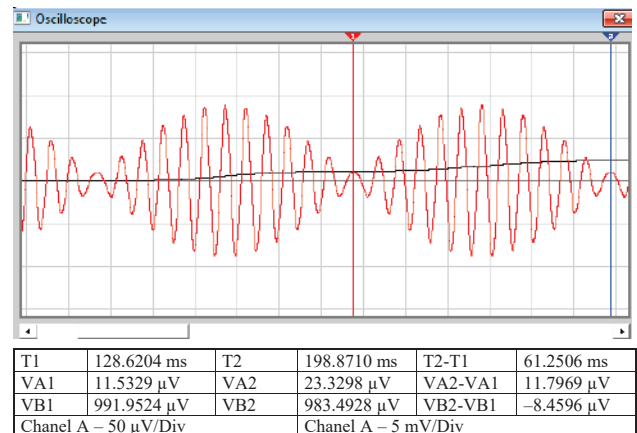| T1	128.6204 ms	T2	198.8710 ms	T2-T1	61.2506 ms
VA1	11.5329 µV	VA2	23.3298 µV	VA2-VA1	11.7969 µV
VB1	991.9524 µV	VB2	983.4928 µV	VB2-VB1	−8.4596 µV
Chanel A – 50 µV/Div			Chanel A – 5 mV/Div		

Fig. 5. Time diagram of the signal of damage to an inner ring

The amplitudes of all output signals in all 3 cases considered above are directly proportional to the intensity of damage.

5. 2. Design of the root-mean-square value detector

On this basis, we constructed the resulting model of the filter's output signal. Fig. 6 presents the functional circuit of RMS detector.

Fig. 7 shows a model of TNF input signal at actual input signals.

The time of analysis T_a should be selected so that it is equal to the period of the minimum beat frequency of the above components, that is: 14.3−8.2=6.1 Hz, then T_a=1/6.1 Hz=164 ms. An increase in the rotor rotation frequency will lead to proportional decrease in the time of analysis, at a maximum frequency of shaft rotation of 142 Hz, the time of analysis T_a=118,4 ms.

To create a model of the signal at the input of RMS detector, we used the appropriate functional elements determined based on the filter's reaction to each frequency, which is responsible for a certain damage.
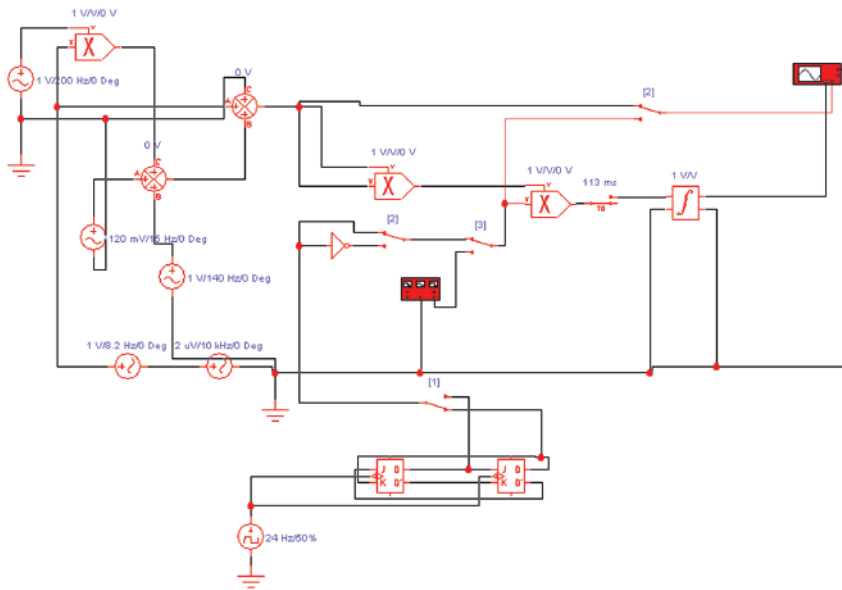
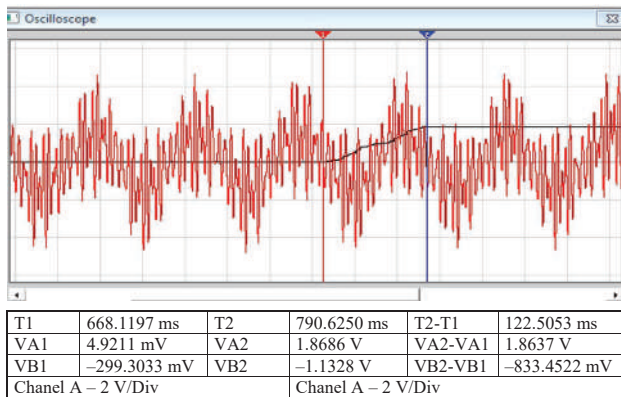Fig. 6. Diagram of RMS detector with a model of the filter's output signal at actual input signals

Table 3

Measurement results

Sample n_1		Sample n_2	
No. of entry	Measurement result	No. of entry	Measurement result
1	1.73036	1	1.73659
2	1.74447	2	1.74398
3	1.73472	3	1.72899
4	1.72782	4	1.73268
5	1.74303	5	1.74485
6	1.73848	6	1.73216
7	1.72676	7	1.72973
8	1.73988	8	1.74415
9	1.74167	9	1.73553
10	1.72722	10	1.72743
m_1	1.73544	m_2	1.73561
s_1	0.0208	s_2	0.0199
n_1	10	n_2	10

T1	668.1197 ms	T2	790.6250 ms	T2-T1	122.5053 ms
VA1	4.9211 mV	VA2	1.8686 V	VA2-VA1	1.8637 V
VB1	−299.3033 mV	VB2	−1.1328 V	VB2-VB1	−833.4522 mV
Chanel A – 2 V/Div			Chanel A – 2 V/Div		

Fig. 7. Result of measuring a signal at the output of RMS detector

5. 3. Result of the method verification using the Student criterion

We shall measure voltage values with an offset in the time interval for two samples of the same size with 10 values each. We estimate, based on the Student criterion, the uniformity, that is, the statistical validity of values variability [22]. We use the t-test with a level of confidence of 95 %.

$$t = \frac{|m_1 - m_2 - d|}{s_o\sqrt{\frac{1}{n_1} + \frac{1}{n_2}}}, \qquad (9)$$

where

$$s_o = \sqrt{\frac{(n_1 - 1)s_1^2 + (n_2 - 1)s_2^2}{n_1 + n_2 - 2}}, \qquad (10)$$

where s_o is the total standard deviation RMS; m_1 and m_2 are the average arithmetic values for each sample; d is the difference between magnitudes that take the test (in this case, $d=0$); n_1 and n_2 is the size of samples ($n_1=n_2=10$).

The estimated value of voltage $U_{RMS}=1{,}7362$ V.

Be calculating formulae (9) and (10), we obtain: $s_o=0.0033$; $t=0.0184$, if we assume $P=0.95$.

The critical value that corresponds to a probability of 95 % of the t-distribution with 18 degrees of freedom: $t_{(0.05\_18)}=2.10$. The test has proven successful because the estimated value is less than the tabular one ($0.018<2.10$). That is, the time of analysis T_a is optimal in order to solve the set task.

5. 4. Investigation and simulation of amplifiers circuits to work with piezoelectric sensors

Another destabilizing factor when employing the piezoelectric sensors is the network interference of general and normal form. Paper [23] proposed eliminating the interferences of general form by using classical circuit of the measuring amplifier based on three operational amplifiers shown in Fig. 8. In this case, a conventional piezoelectric sensor is applied as the sensor. When applying a differential sensor for this circuit, results may prove to be much worse because of the skewness of the sensor itself. The disadvantages of such a solution include a significant penetration of the network voltage via the intra-winding capacity of the power transformer, due to the input links skewness.

In the diagram, the sensor is represented by equivalent voltage generator E1 and capacitance C1. C0 is the capacitance between the wires of a connecting cable. C2, C3 are the parasitic capacitance between the wires of a connecting cable (twisted pair in the screen) and screen. C6 is the parasitic capacitance between the cover of the cable and the ground of the power network. E2 is the equivalent generator of network voltage (110 V, 50 Hz), C7 is the capacitance between windings of the power transformer. Elements E2, C7 form due to the fact that at the network's frequency (50 Hz) the distributed capacitance between the windings of power transformer can be replaced with concentrated capacity (C7) between the middles of windings of the power transformer. Under a balanced variant at C2=C3, C4=C5 and an input voltage of E1=1 V, a signal/noise ratio at the output of the amplifier would be 115 dB.

At the asymmetry of capacities C2, C3 at a level of 10 %, a signal/noise ratio reduces to 4 dB, which makes measurement almost impossible.

Fig. 9 shows the proposed functional circuit of the amplifier to operate with piezoelectric sensors that is devoid of the above-mentioned shortcomings.
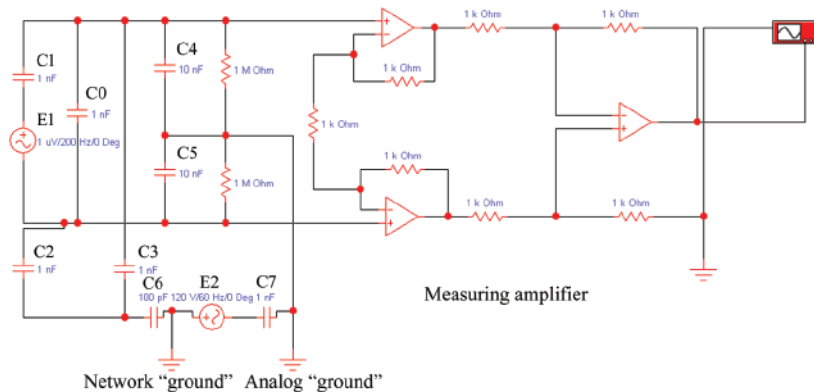
Fig. 8. Model of electrometric measuring amplifier with differential-current inputs for operation with piezoelectric sensors
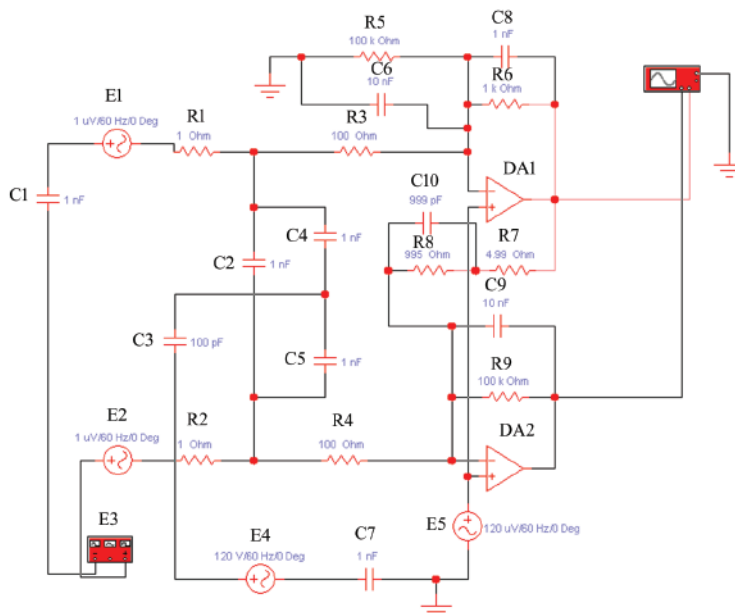

Fig. 9. Model of charge measuring amplifier with differential-current inputs for operation with piezoelectric sensors

The base of the circuit is the measuring charge amplifier with differential-current inputs made on the operational amplifiers DA1, DA2. A piezoelectric sensor is connected to the inputs of this amplifier. In this case, a stage in the amplifier DA1 performs the function of a current inverter, feedback elements R9, S9 form a low-frequency pole of amplifier FR. The output voltage will be equal to ratio:

$$U_{out} = 2e_S \frac{c_S}{c_9}, \qquad (11)$$

where e_S is the equivalent output voltage of the sensor; c_S is the electric capacitance of the sensor; c_9 is the electric capacitor C9.

In order to determine noise-resistance of the amplifier, we constructed a model in the programming environment Electronics Workbench.

The sensor is connected to the measuring amplifier using the cable twisted pair in the screen.

C1 – equivalent capacitance of the sensor.

E3 – equivalent output voltage of the sensor.

That is, the sensor is modeled based on the circuit of an equivalent voltage source: C1, E3.

R1, R2, R3, R4 – the sequential resistances of the cable's wires.

C2 – capacitance between the wires of cables.

C4, C5 – the capacitance between a cable's wire and the screen.

E1, E2 – equivalent generators of voltage to the interference of normal form induced in each wire of the cable based on the equivalent circuit described in [24] by external electromagnetic fields.

E4 – equivalent voltage of general form that occurs due to the capacitance between windings of the force power transformers.

C7 – capacitance between windings of the power transformer.

C3 – parasitic capacitance between the cover (screen) of the input cable and the network ground.

E5 – equivalent source of common form, which occurs due to the general resistances of grounding links.

C10, R8, R7 – adjustment chain for the non-ideal frequency characteristic of DA1.

The current inverter is made on the operating amplifier DA1; in this case, R6≈R7+R8, C8 is the correction capacitance to block the excitation. Elements R9, C9 function to decouple the inputs of operational amplifier DA2 for DC current and form the low-frequency pole of FR. Correction link DA1, R5, C6 is selected so that R5=R9, and C6=C9 to neutralize the influence from source E5.

Similar to the previous case, we determined a signal/noise ratio at the output of the amplifier of penetration of network interference from sources E4 on the output of the amplifier at a 10 % imbalance of capacitance of input cable C4, C5 and determined that it is –30 dB. It is 26 dB larger than in the previous amplifier shown in Fig. 8.

---

6. Discussion of results of investigating the system, 4-channel filter, the resulting output signal, and the measuring amplifier

The proposed system makes it possible to solve the task on early diagnosis of bearing assemblies in GTE even under more adverse operating conditions. It is achieved by applying the tracking notch filters based on N-channel structures, namely a 4-channel filter. The filter has a coefficient of window overlap $k=1$ and is based on the iterative-integrating converters that provide the depth of FR drop at rotor harmonics of up to 120–140 dB [25]. This ensures a signal to noise ratio at the output of the filter of the order of 60 dB at the signal/noise ratio at the input of the filter of –40 dB. Synchronization of the N-channel TNF is executed based on the stable rotor frequency, which makes it possible to detect low-power signals of bearing damage with fluctuating frequencies at a distance of a few percent of the rotor frequency. Solving this issue by applying the tracking narrow-band selective filters is related to the need to employ the synchronization of the tracking filter based on the fluctuating frequency of bearing's damage. The application of the tracking narrow-band filters of high orders is problematic because of the need to measure frequency with high accuracy and over a short time.

We have investigated effectiveness of the proposed method and the device by modeling the damage to an actual GTE bearing. We proposed a procedure for analysis and a generalized vibrodiagnostic criterion which makes it possible to take into consideration the degree of GTE load, which improves accuracy of the preliminary analysis. Its suitability has been demonstrated by testing uniformity of the samples based on the Student criterion.

We have investigated characteristics of the electrometric measuring amplifier to be used with piezoelectric sensors. We have proposed the charge measuring amplifier to be used with piezoelectric sensors under conditions of imbalance of the input link, predetermined by the non-identity of parasitic capacitance of the input cable. It has been shown that the penetration of a network interference to the output of the charge amplifier ensures a better signal/noise ratio than that in the measuring amplifier by 26 dB.

This analysis was carried out without taking into consideration the imbalance of normalizing capacitance of the measuring electrometric amplifier and the impedance of the output differential amplifier. The charge measuring amplifier does not require the balance of capacitance, which is another advantage of such a solution. Suppression of the phase signal in the measuring amplifier with differential-current inputs is carried out by a differential amplifier. It is problematic to combine in one cascade the functions of filtering and amplification, since it requires using two identical capacitors of significant capacitance (tens of nF) with high accuracy. That makes it possible for the charge amplifier to simultaneously perform filtering operation, which in turn would improve the signal/noise ratio at the output by 15–20 dB compared to the electrometric measuring amplifier.

We have developed and applied a new type of tracking N-channel filters based on the iterative-integrating converters with dynamic storage devices, which make it possible to improve accuracy and performance speed of vibrodiagnosis of bearing assemblies. High metrological characteristics are predetermined by the precision of iterative-integrating transducers whose transmission coefficient does not depend on the capacity of the integrator and instrumental errors of analog voltage storage devices, because the principle of operation of an iterative-integrating converter implies that it is a compensator of the astatic type.

A significant disadvantage of the iteratively-integrating transducer is the problem of convergence of the transition process. This means that the time constant of the integrator in feedback should be not less than the period of the second harmonic of the minimum frequency of the input signal. At a strict limitation of the working frequency range, it is possible to avoid the loss of stability by applying a frequency discriminator. In this case, instead of the input signal, the input of the converter will receive the signal with a minimum working range frequency, which is advisable at a narrow band of frequencies of the input signal. Over a wide range of frequencies, it would be more appropriate to automatically, gradually or smoothly, control the constant of the integrator time in accordance with a change in the frequency of the input signal. Over an ultra-low frequency range, it would be appropriate to transfer the spectrum to the high-frequency region, which can also be performed using the iterative-integrating converter.

---

7. Conclusions

1. We have designed a structural circuit for the device that would enable early diagnosis of bearing assemblies. Its special feature is the use of the tracking N-channel notch filter based on the iterative-integrating converters.

2. A procedure for determining the time of analysis for actual input signals has been devised. It is shown that the optimal analysis time for a bearing of type (222) is $T_a=164$ ms, which is one to two orders of magnitude better than that in the standard vibrodiagnostic equipment.

3. We have developed a circuit for the charge amplifier, which, due to the use of differential current inputs, makes it possible to more effectively suppress the interferences of normal and general form at one stage. That improves the signal/noise ratio by 26 dB at the output of the amplifier compared to existing ones under identical conditions.

References

1. Smirnov V. A. Vibracionnaya diagnostiki podshipnikov kacheniya dvigatelya NK-12ST gazoperekachivayushchego agregata GPA-C-6,3. URL: http://www.vibration.ru/12nks/12nks.shtml

2. Ravliuk V. H. Vibrodiahnostyka ta metody diahnostuvannia pidshypnykiv kochennia buksovykh vuzliv vahoniv // Sbornik nauchnyh trudov Doneckogo instituta zheleznodorozhnogo transporta. 2010. Issue 21. P. 177–189.

3. Monitorizaciya mekhanicheskih kolebaniy mashinnogo oborudovaniya. Perevod tekhnicheskogo obzora No. 1. Nerum, 1987.

4. Frariry J. L. Pitfalls in the Analysis of Machinery Vibration measurement // Sound and Vibration. 2002. P. 18–24.

5. Bilosova A., Bilos Ya. Vibracionnaya diagnostika. Ostrava, 2012. 113 p.

6. Azovtsev A. Y., Barkov A. V., Carter D. L. Improving the accuracy of rolling element bearing condition assessment. URL: http://www.vibrotek.com/articles/abcvi96/abcvi96.htm

7. Rutkovskiy V. Yu., Suhanov V. M., Glumov V. M. Sistema izmereniya parametrov radial'nyh vibraciy vala gazoturbinnoy ustanovki // Datchiki i sistemy. 2007. Issue 8. P. 2–7.

8. Patyukov V. G. Fil'traciya signalov chastotnyh datchikov // Datchiki i Sistemy. 2003. Issue 5. P. 2–4.

9. Herris F. Dzh. Ispol'zovanie okon pri garmonicheskom analize metodom diskretnogo preobrazovaniya Fur'e // TIIER. 1978. Issue 1. P. 60–67.

10. Marchenko B. G., Myslovich M. V. Vibrodiagnostika podshipnikovih uzlov elektricheskih mashin. Kyiv: «Naukova dumka», 1992. 196 p.

11. Babak S. V., Myslovich M. V., Sysak R. M. Statisticheskaya diagnostika elektrotekhnicheskogo oborudovaniya: monografiya. Kyiv, 2015. 456 p.

12. Chen A., Kurfess T. R. A new model for rolling element bearing defect size estimation // Measurement. 2018. Vol. 114. P. 144–149. doi: https://doi.org/10.1016/j.measurement.2017.09.018

13. Study on rolling bearing on-line reliability analysis based on vibration information processing / Ying Y., Li J., Chen Z., Guo J. // Computers & Electrical Engineering. 2018. Vol. 69. P. 842–851. doi: https://doi.org/10.1016/j.compeleceng.2017.11.029

14. Schmidt S., Heyns P. S., Gryllias K. C. A discrepancy analysis methodology for rolling element bearing diagnostics under variable speed conditions // Mechanical Systems and Signal Processing. 2019. Vol. 116. P. 40–61. doi: https://doi.org/10.1016/j.ymssp.2018.06.026

15. Bearing diagnostics using image processing methods / Klein R., Masad E., Rudyk E., Winkler I. // Mechanical Systems and Signal Processing. 2014. Vol. 45, Issue 1. P. 105–113. doi: https://doi.org/10.1016/j.ymssp.2013.10.009

16. Smith W. A., Randall R. B. Rolling element bearing diagnostics using the Case Western Reserve University data: A benchmark study // Mechanical Systems and Signal Processing. 2015. Vol. 64-65. P. 100–131. doi: https://doi.org/10.1016/j.ymssp.2015.04.021

17. Seimert M., Gühmann C. Vibration based diagnostic of cracks in hybrid ball bearings // Measurement. 2017. Vol. 108. P. 201–206. doi: https://doi.org/10.1016/j.measurement.2017.03.001

18. Optimised Spectral Kurtosis for bearing diagnostics under electromagnetic interference / Smith W. A., Fan Z., Peng Z., Li H., Randall R. B. // Mechanical Systems and Signal Processing. 2016. Vol. 75. P. 371–394. doi: https://doi.org/10.1016/j.ymssp.2015.12.034

19. Fault diagnosis method based on integration of RSSD and wavelet transform to rolling bearing / Chen B., Shen B., Chen F., Tian H., Xiao W., Zhang F., Zhao C. // Measurement. 2019. Vol. 131. P. 400–441. doi: https://doi.org/10.1016/j.measurement.2018.07.043

20. Dovhan V. V., Ornatskyi D. P. Prystriyi dlia vibrodiahnostyky pidshypnykovykh vuzliv: Pat. No. 60405 UA. MPK: G01M 13/04. No. u201008439; declareted: 06.07.2010; published: 25.06.2011, Bul. No. 12.

21. Karasev V. A. Maksimov V. P., Sidorenko M. K. Vibracionnaya diagnostika gazoturbinnyh dvigateley. Moscow: Mashinostroenie, 1978. 132 p.

22. Teoreticheskie osnovy informacionno izmeritel'nyh sistem / Babak V. P., Babak S. V., Eremenko V. S., Kuc Yu. V., Marchenko N. B., Mokiychuk V. M. et. al.; V. P. Babak (Ed.). Kyiv, 2014. 832 p.

23. Makarenko V., Chermyanin A. Maloshumyashchiy usilitel' dlya p'ezokeramicheskih datchikov // Elektronnye komponenty i sistemi. 1999. Issue 5 (21).

24. Barns Dzh. Elektronnoe konstruirovanie: Metody bor'by s pomekhami. Moscow: Mir, 1990. 238 p.

25. Ornatskyi D., Dovhan V. Doslidzhennia parametriv N-kanalnykh filtriv dlia vibratsiynoho analizu pidshypnykovykh chastot // Metrolohiya ta prylady. 2018. Issue 1. P. 46–52.